Hindawi
International Transactions on Electrical Energy Systems
Volume 2022, Article ID 3307679, 11 pages
https://doi.org/10.1155/2022/3307679

Research Article

A Bayesian Multiobjective Approach Based on GMPPT for PV Arrays

Sharareh Noroozi, Heidarali Shayanfar, and Mehrzad Nasirian

Department of Electrical Engineering, Islamic Azad University South Tehran Branch, Tehran, Iran

Correspondence should be addressed to Sharareh Noroozi; sharareh.noruzi@gmail.com

Received 14 December 2021; Revised 2 May 2022; Accepted 6 June 2022; Published 29 June 2022

Academic Editor: Santi A. Rizzo

This paper considers the problem of tracking the global maximum power point (GMPP) in partially shaded conditions (PSCs) as a multiobjective optimization problem and solves it using a novel multiobjective optimization algorithm on the basis of Bayesian optimization formulation. Bayesian optimization is a metamodel-based global optimization method that is able to balance exploration and exploitation. The Pareto solutions are obtained by using a multiobjective Bayesian optimization algorithm. Also, a new acquisition function is proposed to improve the diversity and convergence of the Pareto solutions. Two objective functions are introduced to remove the large tracking errors and oscillations of the operating point around the GMPP. The suggested method is implemented online for GMPP tracking so that the suggested method monitors any change in environmental conditions and generates the optimal duty cycle for the DC-DC converter for the GMPP tracking (GMPPT) by the PV array. Several multipeak PSC scenarios are implemented and simulated to show efficiency of the suggested approach. The MATLAB/SIMULINK is employed to implement a photovoltaic (PV) system comprising a PV array, a boost converter, and the proposed multiobjective Bayesian optimization algorithm (MOBOA). The simulation results show a very satisfactory performance of the MOBOA in terms of transient state and steady-state oscillations and tracking speed.

1. Introduction

With growing concerns about the degradation of the environment by fossil fuels, the importance of renewable energy sources has become much more apparent to researchers and policymakers today than ever before [1]. PV modules are a viable alternative to conventional fossil energy sources, taking into account ease of operation, low maintenance, perpetual sunlight, and constant price reductions. However, large-scale implementation of solar farms still requires high investment costs [1]. In addition, weather conditions greatly affect the performance of PV modules. To reduce these shortcomings, two solutions have been suggested: the use of improved silicon semiconductors in the fabrication of PV modules and the use of a maximum power point tracker to increase the efficiency of PV arrays. The second solution requires much less cost than the first solution [2]. The principal purpose of the second solution is to operate the PV array with the highest efficiency. To operate the PV arrays at the MPP, methods such as perturb and observe (P&O) [3], hill climbing (HC) [4], and incremental conductance (IC) [5] were suggested as the most common traditional MPP tracker. The benefits of these trackers are easy implementation and uncomplicated structure. However, in the event of partial shading or rapid changes in the irradiation, their performance is impaired, and they reduce the efficiency of the PV array. The power fluctuations, deviation from the MPP, and consequent increase in the losses dramatically decrease the PV array efficiency [6].

Considering advantages such as efficiency, precision, fault tolerant, and speed of progress, MPP trackers based on artificial intelligence (AI) can be considered as a trustworthy alternative to traditional MPP trackers methods [7, 8]. Various techniques of the AI-based MPPT such as fuzzy logic (FL) [9–11], neural networks (NNs) [12, 13] and PSO [14, 15], firefly [16], genetic algorithm [17], pattern search

[18], modified bat algorithm [19], bio-inspired memetic salp swarm algorithm [20], hybrid whale optimization-simulated annealing algorithm [21], wind-driven [22], musical chair algorithm [23], following optimization [24], and spotted hyena optimization algorithm [25] have been effectively performed and implemented as an MPPT. However, the main drawback of these methods is transient oscillations, which reduce the efficiency of PV systems.

One of the most important branches of artificial intelligence is neural networks that have different uses in MPPT studies. To estimate the voltage value at the maximum power point, an artificial neural network has been used in [26]. In this regard, the neural network is trained by a big dataset including the radiation level and the voltage value at several MPPs. Thus, the neural network can understand the relationship between the radiation level and the voltage value at the MPP. The neural network is then used to generate the duty cycle of a DC-DC converter. In [27], the duty cycle of a DC-DC converter is directly generated by a neural network MPPT. Regardless of suitable performance, the main drawbacks of employing neural networks are the time-consuming training process, overfitting, and so on [26–28]. On the other hand, simple structure and implementation can be mentioned as the benefits of the FL controller, while dependence on the knowledge of the designer can be declared to be the main problem [29–32].

In several articles, hybrid MPPT methods have been suggested. These methods combine the proper offline training and online process. This type of method is a combination of optimization algorithms such as particle swarm optimization [33–37] and a genetic algorithm [38, 39] with artificial intelligence methods such as the fuzzy logic [40–43] and neural network [44–47]. A number of papers use different kinds of optimization algorithms to control multiple PV modules [34] to optimize the classical HC algorithm [35] and to optimize the P&O algorithm [48]. Again, the main problem of these approaches is transient oscillations.

In [49], the Bayesian fusion is used to help the controller avoid falling into the local minimum trap of the P-V shaded curve. In [49] a dragonfly optimization algorithm (DOA) is proposed to extract the MPPT in PV systems. Again, the main drawback of these methods is transient oscillations.

The main objectives in MPPT design are as follows: MPP tracking, minimum steady-state oscillations, and minimum transient oscillations. MPPTs based on optimization algorithms need an objective function to achieve the above objectives. All of MPPT methods have so far used a single-objective function that may not include all the important information in the system. Therefore, it is necessary to use more than one objective function to achieve all design objectives. This paper formulates the problem of the PSC with minimal steady and transient oscillations and rapid convergence into a multiobjective function and solves it with a novel multiobjective optimization algorithm. To cancel the oscillations around the MPP in transient and steady states and to remove the large tracking errors, two objective functions are proposed. The proposed MOBOA generates the optimal duty cycle to minimize these two objective functions.

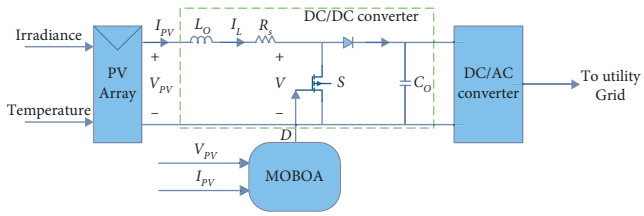

Figure 1: The configuration of the PV system.

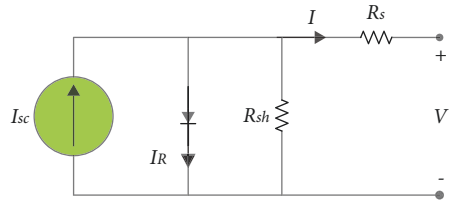

Figure 2: The equivalent circuit of the single photovoltaic cell.

In section 2, a PV system is described briefly. In section 3, the objective functions are provided to design an MPPT. In section 4, the multiobjective Bayesian optimization algorithm is presented in detail. Section 5 presents detailed simulation results.

2. System under Study

Different types of PV systems are proposed in the literature to evaluate MPPT algorithms such as grid tied, standalone grid [50], and grid/hybrid [51]. In this paper, the grid-tied type of PV systems is used. The general block diagram of a PV system is shown in Figure 1. As seen in this figure, this system consists of a PV array, the suggested MOBOA, a DC-DC converter, and a DC/AC converter [52, 53]. A PV array is connected to a utility grid through a DC-DC converter and a three-phase three-level voltage source converter (VSC). The DC-DC converter is controlled by the proposed GMPPT which is the proposed MOBOA in this paper, and the DC voltage is then converted into the AC voltage by using the DC/AC converter.

3. Mathematical Modeling of the Single PV Cell

Figure 2 plots a solar cell equivalent circuit that is modeled by

$$V = \frac{nKT}{q}\ln\left(\frac{I_{sc}}{I} + 1\right), \tag{1}$$

$$I = I_{sc} - I_R\left[\exp\left(\frac{q(V + IR_S)}{nKT}\right)\right] - \frac{V + R_S I}{R_{sh}}, \tag{2}$$

where I_{sc} is the short-circuit current of the PV array, T is the cell temperature, I_R is the reverse saturation current, I_{sc} is the short-circuit current of the PV cell, q is the electronic charge, K is the Boltzmann constant, n is the diode ideality factor, R_{sh} is the resistance in parallel, R_s is the resistance in series, V is the PV cell voltage, and I is the PV cell current.

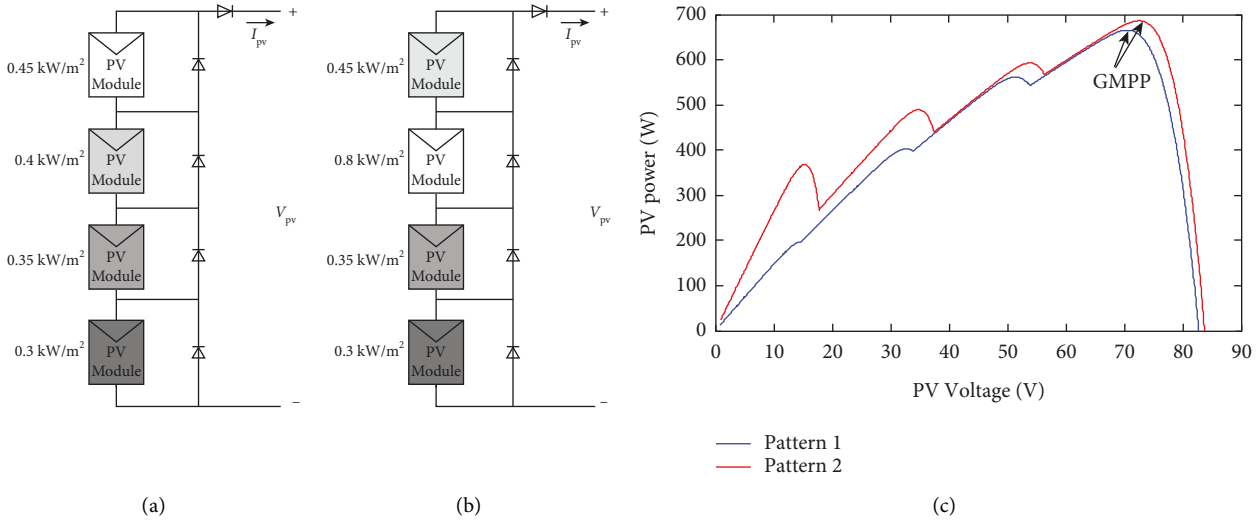

Figure 3: Four PV modules in series: (a) partial shading pattern 1, (b) partial shading pattern 2, and (c) P-V curve of the PV array.

4. Partial Shading Conditions

PV modules are usually connected in different configurations to increase voltage and current of the PV array. Due to the presence of bypass diodes, the occurrence of the PSC creates a number of global and local peaks in the P-V curve of the PV array. Figures 3(a), 3(b) and 3(c) show an arrangement including four PV modules in series with two various shading patterns along with their P-V curves, respectively.

5. Objective Functions to Design an MPPT

The main objectives in MPPT design are as follows: MPP tracking, minimum steady-state oscillations, and minimum transient oscillations. MPPTs based on optimization algorithms need an objective function to achieve the aforementioned objectives. All of MPPT methods have so far used a single-objective function that may not include all the important information in the system. Therefore, it is necessary to use more than one objective function to achieve all design objectives. In this paper, two objective functions are proposed to design an MPPT controller using the MOBOA. The first objective function is the integral squared error (ISE) and the second one is the integral of time-weighted absolute error (ITAE). Minimizing the ISE leads to removal of the large tracking errors caused by sudden changes in irradiance. Minimization of the ITAE will reduce oscillations around the MPP. The objective functions can be formulated as follows:

$$ISE = \int_0^t \left(\frac{dP_{PV}(\tau)}{dV_{PV}(\tau)}\right)^2 d\tau, \tag{3}$$

$$ITAE = \int_0^t \tau \left|\frac{dP_{PV}(\tau)}{dV_{PV}(\tau)}\right| d\tau, \tag{4}$$

where V_{PV} and P_{PV} are the PV array voltage and PV array power, respectively.

6. MOBOA and Its Application in the Design of MPPT

It is necessary to use the MPP tracker to increase the efficiency of the PV system under different environmental conditions. In this section, a method for GMPP tracking in PV systems under different radiation patterns is introduced.

6.1. Multiobjective Optimization. The following equation presents a general structure of multiobjective optimization problems:

$$\begin{aligned} &\min_x F(x) = \{f_1(x), f_2(x), f_i(x)\} \\ &\text{s.t.} \quad g_j(x) \le 0, \quad j = 1, 2, \ldots, n \\ &\qquad x_{lb} \le x \le x_{ub}, \end{aligned} \tag{5}$$

where $F(x)$ includes a vector of individual objective functions, $g_j(x)$ is the constraint, and x_{ub} and x_{lb} denote the upper and lower bounds. Due to trade-offs between the objective functions, the multiobjective optimization problem given in (5) usually has a set of optimal solutions in the Pareto sense. In other words, there is no optimal solution that is superior to other solutions. That is, there is no optimum solution that is superior to the other in terms of all objectives [54].

6.2. The Kriging Model. Bayesian optimization usually uses the Kriging or Gaussian process regression model. In general, the Kriging model can be expressed as the surrogate of the expensive function $f(x)$ as a realization of a stochastic process $Y(x)$.

$$Y(x) = \mu + Z(x). \tag{6}$$

In which, $Z(x)$ and μ denote the error and mean term of the Gaussian process, respectively. Here, the simple Kriging model is utilized and $Z(x)$ follows a normal distribution with the nonzero covariance and zero mean and μ is a fixed value.

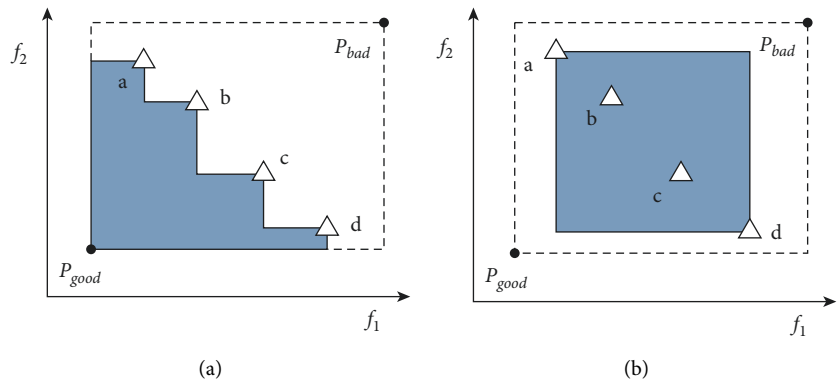

Figure 4: The quality metrics: (a) RHD; (b) OS. The RHD and OS for the current Pareto set $P = \{a, b, c, d\}$ are computed.

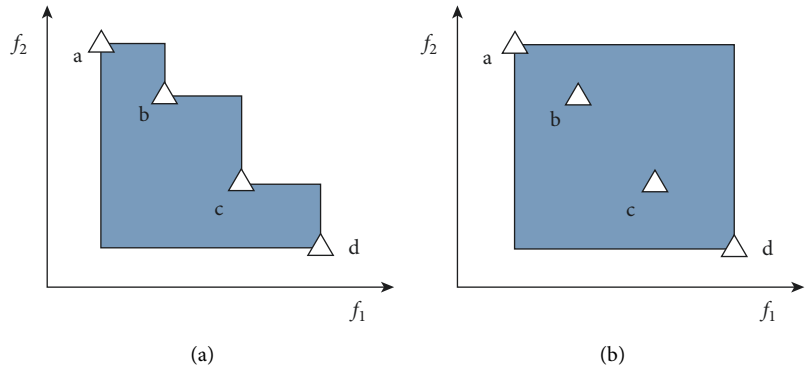

Figure 5: The modified quality metrics: (a) MHD; (b) MOS.

The following equation represents the Gaussian spatial correlation function between the values of function f at two locations x and x':

$$\operatorname{cov}\left(Z(x), Z(x')\right) = \sigma^2 \rho(x, x') = \sigma^2 \exp\left\{-\sum_{j=1}^{u} \theta_j \left(x_j - x_j'\right)^2\right\}, \tag{7}$$

where $\sigma 2$ is the standard deviation and θj is the roughness parameter. Reference [55] provides more detail about the Kriging model.

6.3. Bayesian Optimization. In the Bayesian optimization for the global optimization, the Kriging model is used to approximate the unknown objective function $f(x)$. For a trade-off between exploration and exploitation in the searching process, an acquisition function is used. In this paper, the lower confidence bound (LCB) is considered as the acquisition function. The LCB acquisition function can be expressed as follows:

$$f_{LCB}(x) = \widehat{f}(x) - ks(x), \tag{8}$$

where $f'(x)$ is the Kriging model, $s(x)$ represents the square root of the mean squared error, and k denotes the exploitation-exploration balance. A new sample point generated by minimizing the LCB acquisition function updates the Kriging model.

6.4. The Suggested MOBOA. To define the new acquisition function, the suggested MOBOA modifies two metrics for the quality of the Pareto set, overall spread (OS) and the relative hyperarea difference (RHD).

6.4.1. The Modified Metrics. The quality of Pareto frontiers is usually measured by the RHD and OS [56]. In Figure 4, the diversity and convergence of the obtained Pareto frontier are represented by the OS and RHD, respectively. The RHD and OS are the polygon area formed by the Pareto frontier and the bounding box of the frontier, respectively. If the RHD value is small, the convergence of the Pareto frontier will be higher. Moreover, if the OS value is large, the diversity of the Pareto frontier will be higher.

$$RH\ D = \frac{HA\left(P_{\text{bad}}, P_{\text{good}}\right) - HA\left(P_{\text{bad}}, a, b, c, d\right)}{HA\left(P_{\text{bad}}, P_{\text{good}}\right)}, \tag{9}$$

$$OS = \frac{HA\left(\text{extremes}(P)\right)}{HA\left(P_{\text{bad}}, P_{\text{good}}\right)}, \tag{10}$$

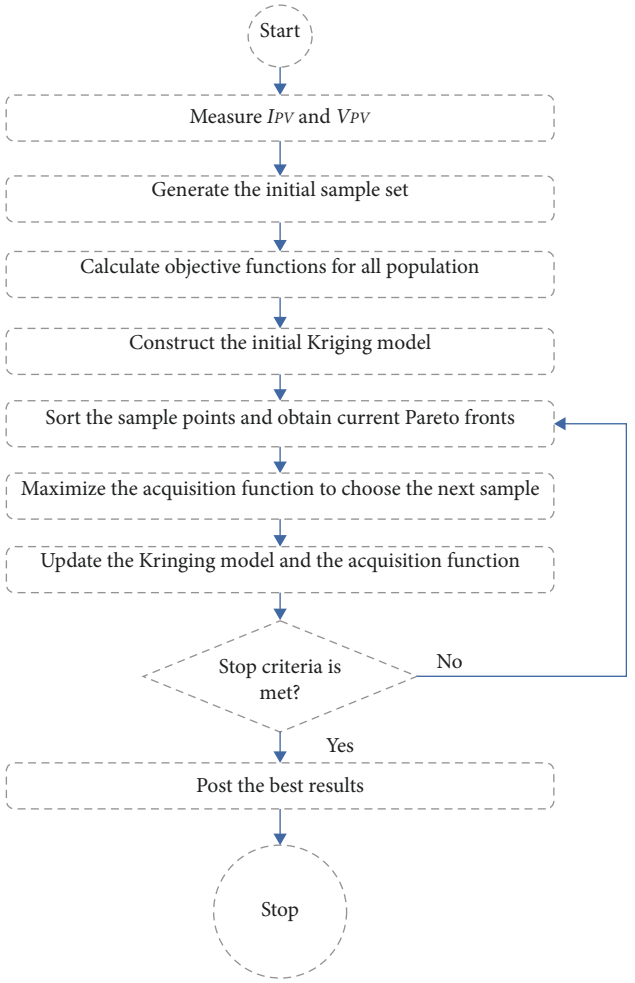

Figure 6: The flowchart of the suggested approach.

Table 1: PV cell specifications.

Description	Value
Voltage at Pmax (Vmp)	5 V
Current at Pmax (Ipm)	0.8 A
Open circuit voltage (VocN)	6 V
Short-circuit current (ISC)	0.9 A
Temperature coefficient of voltage (Kv)	$-6 \times 10{-}3$ V/K
Temperature coefficient of current (Ki)	$5.4 \times 10{-}4$ A/K
Surface emissivity (εs)	0.8
Surface area	0.2 mm × 0.2 mm

where P_{good} is a good solution, P_{bad} is a much worse solution than the frontier, $HA(extremes(P))$ is the hyperarea bounded by the two extreme points in the Pareto frontier, and $HA(P_{\text{bad}}, P_{\text{good}})$ is the area of the bounding box formed by P_{bad} and P_{good}.

The key drawbacks of the OS and RHD are as follows: (1) P_{good} and P_{bad} must be determined before computing the two metrics and (2) in case of finding a new Pareto between two existing Pareto solutions, the RHD value of the Pareto front increases instead of reducing uniformly. To tackle these drawbacks, the MOBOA uses the modified overall spread (MOS) and the modified hyperarea difference (MHD). In Figures 5(a) and 5(b), the shaded areas indicate the values of the MOS and the MHD.

Table 2: DC-DC converter specifications.

Description	Value
Switching frequency	20 KHz
Capacitor	200 μF
Inductor	0.01 mH

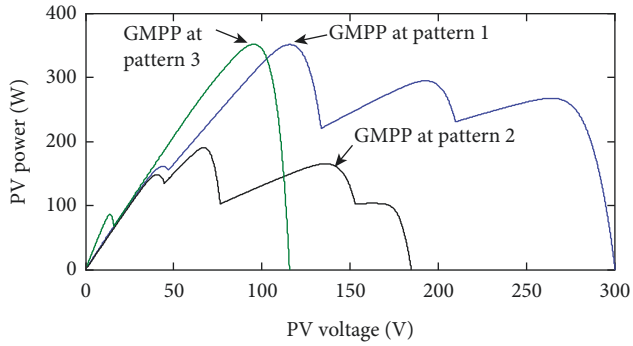

Figure 7: The P-V curve of PSC patterns in Case 1.

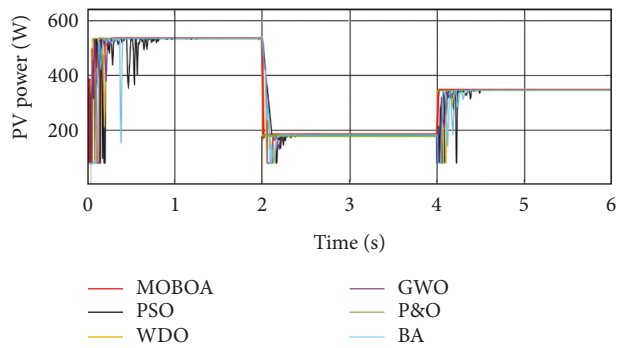

Figure 8: The PV power in the presence of competitive algorithms in Case 1.

6.4.2. The Suggested Acquisition Function. Using the MHD and MOS, new Pareto solutions in the unsearched space are obtained from a new acquisition function. LCB functions are employed to consider the uncertainty related to the objective surrogates to improve the efficiency of the computational functions and robustness. The LCB functions are represented by

$$\mathbf{f}_{LCB}(x) = \left[f_{LCB,1}(x), f_{LCB,2}(x), \ldots, f_{LCB,M}(x)\right], \tag{11}$$

where

$$f_{LCB,i}(x) = \widehat{f}_i(x) - k_i s_i(x), \quad \text{for } i = 1, \ldots, M, \tag{12}$$

where M is the number of objective functions approximated by the Kriging model, $\widehat{f}_i(x)$ is the predicted mean, and $s_i(x)$ is the Kriging model standard deviation for the ith objective function at x.

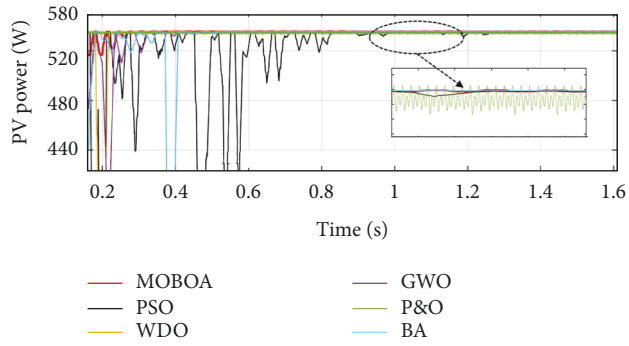

Figure 9: The zoomed-in PV power in Case 1.

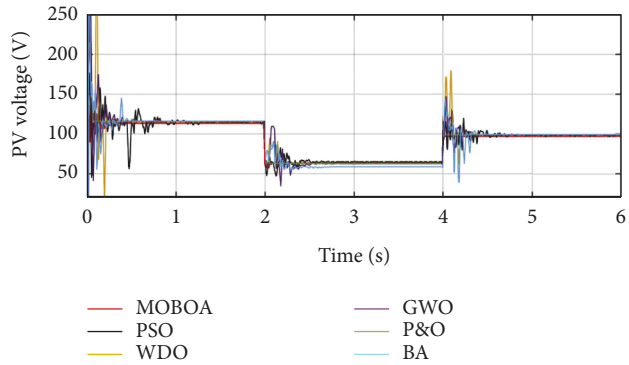

Figure 10: PV voltage in Case 1.

Table 3: A comparative study between the competitive algorithms in Case 1.

Algorithm	Efficiency (%) (using (19))	Quantification of transient oscillations (using Eq. (17))	Quantification of steady-state oscillations (using Eq. (18))	Tracking time (s)	Settling time (s)
MOBOA	99.58	0.66	0.08	0.13	0.25
PSO	89.75	6.98	2.54	0.34	0.84
WDO	98.38	1.93	1.03	0.23	0.38
GWO	97.33	3.11	1.13	0.27	0.54
P&O	85.32	0.30	6.82	0.14	0.39
BA	94.99	4.27	1.66	0.22	0.55

The goal of the suggested acquisition function is to obtain a solution to maximize the quality of the Pareto solutions. The diversity or convergence of the Pareto set can always be improved by Pareto's new solution. Therefore, the suggested acquisition function can be expressed as

$$a(x) = \max\left(I_{MH\ D}(x), I_{MOS}(x)\right), \tag{13}$$

where

$$I_{MHD} = \left|\frac{MH\ D(\{D_n, x\}) - MH\ D(D_n)}{MH\ D(D_n)}\right|, \tag{14}$$

$$I_{MOS} = \left|\frac{MOS(\{D_n, x\}) - MOS(D_n)}{MOS(D_n)}\right|, \tag{15}$$

where Dn is n existing sample points, MHD(D_n) is the MHD based on D_n and MOS(D_n) is MOS based on D_n, and MHD($\{D_n, x\}$) and MOS($\{D_n, x\}$) are the updated MHD and MOS in case of adding x into the sample set. By maximizing Eq. (13), the Kriging models are updated by a new sample point.

7. Result and Discussion

Now, several scenarios are simulated to justify the effectiveness of the MOBOA in tracking the GMPP. In addition, the following equation is used to compute the efficiency of the PV array:

$$\eta = \frac{\sum_{k=1}^{N} P_{MPPT} \times T_s}{\sum_{k=1}^{N} P_{GMPP} \times T_s}, \tag{16}$$

where PMPPT and PGMPPT are the output power of the PV array and the global maximum power, respectively and Ts is the sampling time.

In addition, to assess the performance of algorithms, the following criteria called quantification of transient oscillations indicating the power loss with respect to the GMPP are utilized:

$$P_{tr_{\text{loss}}} = \int_0^{t_{\text{conv}}} (G - P(\tau))\mathrm{d}\tau, \tag{17}$$

where G is the PV power at the GMPP, P is the instantaneous PV power and tconv is the convergence time of the algorithm at the GMPP. In addition, the following criteria for quantifying the steady-state error (SSE) are introduced:

$$P_{SS_{\text{loss}}} = \int_{t_{conv}}^{t_s} (G - P(\tau))\mathrm{d}\tau, \tag{18}$$

where t_s is the time simulation.

Figure 6 shows the flowchart of the suggested approach to track the GMPP using the MOBOA.

Simultaneous satisfaction of the following conditions terminates the optimization algorithm:

(1) When the difference between the current and previous quality criteria is less than a certain value (e.g., 2% in this study), or the number of iterations reaches a predetermined maximum value, (in this study, maximum value is 30).

(2) When at least k solutions are found by the optimization algorithm so that a sufficient number of the Pareto solutions give sufficient choices to the decision maker. Here, k is selected to be 15.

To validate the ability of the suggested approach, the performance of the suggested method is compared with the results acquired from PSO, WDO [22], GWO [57], P&O, and BA.

The parameters used in the simulations are presented in Tabels 1 and 2.

7.1. Case Study 1: Fast Varying Irradiance Profile. In Case 1, a fast varying irradiance profile at the constant temperature shown in Figure 7 is radiated to the PV array to detect the impact of fast changes in irradiance and the ability of the different MPPT algorithms to track and retrack the GMPPs. In Figure 8, from the power analysis, it can be concluded that the PV system produces a power of 536 W with an efficiency of 99.97% at the presence of the proposed algorithm, which is the highest power extracted from the PV array at the time interval of $t = 0$ to $t = 2$ s. Also, the PV system in the presence of PSO, WDO, GWO, P&O, and BA generates 534.8 W, 535.2 W, 535.6 W, 532.8 W, and 535.2 W at the steady state, respectively. Figure 9 shows the zoomed-in PV power for the time interval of $t = 0.2$ s to $t = 1.6$ s. In Figure 10, the PV voltage is plotted for different algorithms. As seen in this figure, the algorithms of PSO and BA generate large oscillations at the transient state. In the steady state, the step size of the P&O generates large oscillations around the GMPP with an amplitude of nearly 10 W.

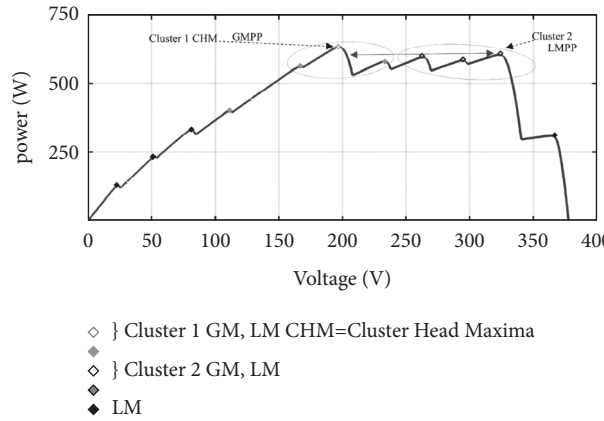

Figure 11: The P-V curve of the PV system in Case 2.

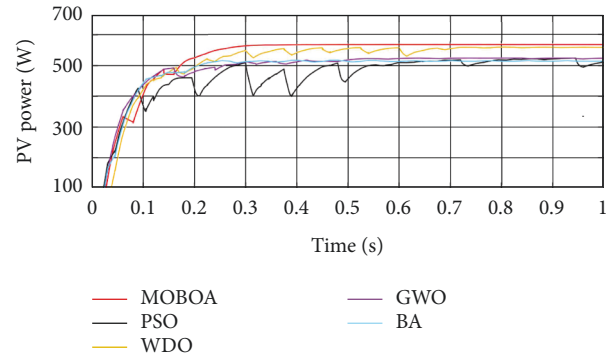

Figure 12: The PV power in the presence of competitive algorithms in Case 2.

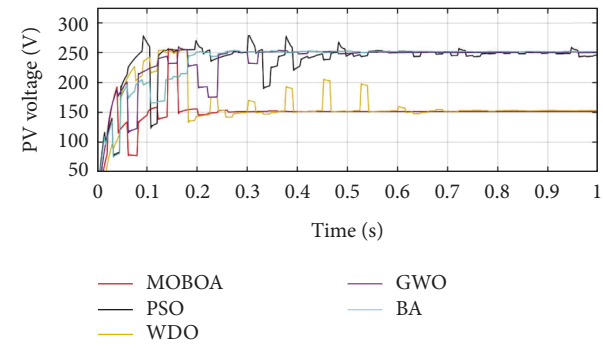

Figure 13: The PV voltage in the presence of competitive algorithms in Case 2.

The average power value of the profile radiated to the PV array in Case 1 is 356.26. The average power generated by MOBOA, BA, P&O, GWO, WDO, and PSO is 352.76, 345.56, 331.44, 345.44, 344.48, and 342.24 W, respectively. The performance of the MOBOA in tracking and retracking the GMPP is highly efficient and robust to fast changes in the irradiance. The P&O algorithm has undesirable oscillations around the GMPP.

Table 4: A comparative study between the competitive algorithms in Case 2.

Algorithm	Efficiency (%) (using (19))	Quantification of transient oscillations (using Eq. (17))	Quantification of steady-state oscillations (using Eq. (18))	Tracking time (s)	Settling time (s)	Algorithm complexity
MOBOA	99.87	0.29	0.03	0.21	0.40	Relatively high
PSO	93.32	4.22	1.81	0.43	1.01	Average
WDO	98.84	1.03	0.67	0.35	0.80	Average
GWO	92.45	3.93	1.72	0.32	0.64	Average
BA	91.61	5.88	2.14	0.34	0.54	Relatively high

The performance of competitive techniques is discussed by two characteristics, settling time and tracking time. Most optimization algorithms strike a balance between the settling time and the tracking time which is carried out by separating the procedure into phases of the exploration and exploitation. Table 3 compares the results obtained from different algorithms in terms of efficiency, quantification of transient oscillations, tracking time, and settling time.

7.2. Case Study 2: Complex Partial Shading Conditions. In Case 2, a PV system having 12 similar series-connected panels is selected to evaluate the performance of competitive algorithms under complex partial shading conditions with the P-V curve shown in Figure 11. Due to the wide distribution of partial shading, local maximum power points are created in the form of clusters. The maximum power point of the cluster is known as the cluster head maximum (CHM). As seen in Figure 11, there are two distinct clusters called cluster 1 in the left half of the P-V curve having four maximum power points and cluster 2 in the right half of the P-V curve having three maximum power points. The global maximum power point or the CHM is located in cluster 1 and is close to the local maximum power point of cluster 2.

In cluster 1, the GMPP is located at 666 W and 198 V, and in cluster 2, the CHM lies at 618 W and 324 V. In cluster 1, the mean power is 616.3 W and the mean power of cluster 2 is 628.1 W. It means that although the GMPP lies at cluster 1, there is a strong possibility that the particles will move towards cluster 2 and settle at the CHM located in cluster 2.

Figures 12 and 13 compare the PV power and PV voltage obtained from different algorithms, respectively. It is clear from this figure that the PV system generates 665 W in the presence of the MOBOA. The PV system in the presence of algorithms of WDO, GWO, PSO, and BA generates 659 W, 622 W, 621 W, and 614 W, respectively. It is concluded that the algorithms of the MOBOA and WDO are able to recognize the CHM in cluster 1, and the rest of algorithms are trapped at the local maximum power points. Table 4 compares the results obtained from the competitive algorithms in Case 2. Although the algorithms of GWO and BA have less tracking time and settling time than WDO, but these two algorithms are unable to recognize the true CHM. This fact can be deduced from the efficiency value. In addition, the algorithms are compared in terms of algorithm complexity.

7.3. Case Study 3: Fast Changes in Temperature and Irradiation. Variable environmental conditions due to nonlinear properties are a challenging issue for the solar photovoltaic system. The problem of drift is an important problem that arises due to incorrect estimation of the perturbation to increase radiation. Here, the results of the MOBOA are compared with the results of the FOA proposed in [24]. Figure 14 shows the PV power and fast changes in temperature and irradiation. In this case study, from $t = 0$ to $t = 1$ s, temperature is 25°C, irradiation is 400 W/m^2, and the maximum power is 121.5 W; from $t = 1$ s to $t = 2$ s, temperature is 25°C, irradiation is 600 W/m^2, and the maximum power is 198.3 W; from $t = 2$ s to $t = 3$ s, temperature is 30°C, irradiation is 750 W/m^2, and the maximum power is 262.2 W; from $t = 3$ s to $t = 4$ s, temperature is 35°C, irradiation is 900 W/m^2, and the maximum power is 331.7 W. The efficiency of MPPTs is as follows: P&O 87.97%, MOBOA 99.63%, and PSO 97.61%. Table 5 compares the results obtained from the competitive algorithms in Case 3.

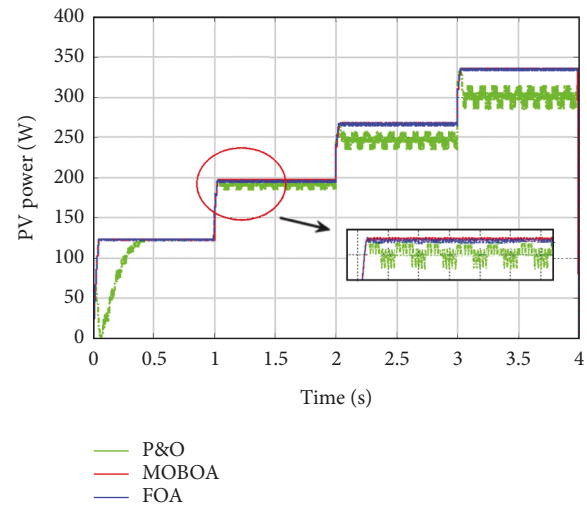

Figure 14: PV power for step change irradiation.

Table 5: A comparative study between the competitive algorithms in Case 3.

Algorithm	Efficiency (%) (using Eq. (19))	Quantification of transient oscillations (using Eq. (17))	Quantification of steady-state oscillations (using Eq. (18))
MOBOA	99.87	0.04	0.02
PSO	99.51	0.04	0.08
P&O	87.97	0.01	10.98

Table 6: Performance summary of MPPT algorithms.

Algorithm	Rise time (ms)	Retracking time (ms)	Transient oscillations	Steady-state oscillations	No. Of adjustable parameters	Ability to handle PSC
MOBOA	100–200	100–150	Low	Zero	10	Yes
WDO	200–300	100–300	Relatively low	Zero	5	Yes
BA	200–500	100–400	Relatively high	Low	8	Failure in some cases
P&O	50–700	50–100	Very low	High	1	No
GWO	230–350	100–400	Relatively low	Low	3	Failure in some cases
PSO	200–500	100–400	Relatively high	Low	3	Failure in some cases

7.4. Discussion. The proposed MPPT based on the MOBOA is able to achieve all objectives of designing an MPPT controller such as accurate MPPT tracking, little steady state, and transient state oscillations. Despite these successes, the main drawback of the proposed approach is its relative complexity.

Table 6 summarizes the ability of the algorithms mentioned in this study to track the GMPP. The tracking speed is selected as the first variable to assess the algorithm performance; the MOBOA seems to be the quickest; considering the speed between 100 ms and 200 ms. The P&O and MOBOA have roughly the same speed. This is because the P&O algorithm only requires a gradual rise from zero to a maximum point with a fixed step size. As the step size increases, the convergence speed increases, but fluctuations around the GMPP occur at the steady state.

In terms of tracking new GMPPs, P&O takes less time to retrack the new GMPP since its performance is only dependent on the gradient of the P-V curve, so it is easier to climb the GMPP. On the contrary, the competitive algorithms are based on search space. When a change in climate occurs, the search-based algorithms scatter their samples all over the P-V curve. In addition, the speed of the tracking is strongly dependent on the random numbers generated. Considering the transient performance, it should be noted that the MOBOA has the quickest algorithms.

Fluctuations around the GMPP lead to energy loss at the steady state. The absence of these oscillations in the transient and steady state can be declared as the key benefit of the MOBOA.

The step size is the only adjustable parameter of the P&O method. Implementing this algorithm is easy and simple.

Obviously, P&O is unable to handle PSCs. This may be critical in a variety of situations, especially for the building of integrated PV systems in crowded areas. The WDO and MOBOA can handle the PSC well. The other algorithms may fail to handle the PSC.

8. Conclusion

This paper suggests a modified bat optimization algorithm to track the global maximum power point in the PV system under different conditions such as load variations, sudden variations of the irradiation level, and partially shaded condition. This method is utilized to directly generate the duty cycle of the boost DC-DC converter. This paper formulates the problem of the PSC with minimal steady and transient oscillations and rapid convergence into a multiobjective function and solves it with a novel multiobjective optimization algorithm. To cancel the oscillations around the MPP in transient and steady states and to remove the large tracking errors, two objective functions are proposed. The proposed MOBOA generates the optimal duty cycle to minimize these two objective functions. The simulation tests are performed to confirm the performance of the suggested method. The results confirm that the suggested controller has a number of benefits: (1) more rapid tracking speed, (2) no oscillations around the GMPP, (3) finding the GMPP for any environmental condition, and (4) the simple implementation of the proposed approach using low-cost microcontrollers.

Abbreviations:

R_s: Series resistance
R_{sh}: Shunt resistance
I_{sc}: Light induced current
V_T: Thermal voltage
N: Diode ideality factor
K: Boltzmann constant
Q: Electronic charge
V_{ref}: Reference voltage.

Data Availability

No data were used to support this study.

Conflicts of Interest

The authors declare that they have no conflicts of interest.

References

[1] M. Taherkhani, J. Faraji, M. Khanjanianpak, E. Aliyan, and M. I. Ghiyasi, "A GMPPT design using the following optimization algorithm for PV systems," *International Transactions on Electrical Energy Systems*, vol. 31, 2021.

[2] W. Zhang, R. Zhu, B. Liu, and S. Ramakrishna, "High-performance hybrid solar cells employing metal-free organic dye modified TiO2 as photoelectrode," *Applied Energy*, vol. 90, no. 1, pp. 305–308, 2012.

[3] Y. Liu, M. Li, X. Ji, X. Luo, M. Wang, and Y. Zhang, "A comparative study of the maximum power point tracking methods for PV systems," *Energy Conversion and Management*, vol. 85, pp. 809–816, 2014.

[4] X. Xiao, X. Huang, and Q. Kang, "A hill-climbing-method-based maximum-power-point-tracking strategy for direct-drive wave energy converters," *IEEE Transactions on Industrial Electronics*, vol. 63, no. 1, pp. 257–267, 2016.

[5] K. Punitha, D. Devaraj, and S. Sakthivel, "Artificial neural network based modified incremental conductance algorithm for maximum power point tracking in photovoltaic system under partial shading conditions," *Energy*, vol. 62, pp. 330–340, 2013.

[6] A. Al-Amoudi and L. Zhang, "Optimal control of a grid-connected PV system for maximum power point tracking and unity power factor," in *Proceedings of the Seventh International Conference on Power Electronics*, London, UK, 1998.

[7] A. Reza Reisi, M. Hassan Moradi, and S. Jamasb, "Classification and comparison of maximum power point tracking techniques for photovoltaic system: a review," *Renewable and Sustainable Energy Reviews*, vol. 19, pp. 433–443, 2013.

[8] T. Esram and P. L. Chapman, "Comparison of photovoltaic array maximum power point tracking techniques," *IEEE Transactions on Energy Conversion*, vol. 22, no. 2, pp. 439–449, 2007.

[9] U. Yilmaz, A. Kircay, and S. Borekci, "PV system fuzzy logic MPPT method and PI control as a charge controller," *Renewable and Sustainable Energy Reviews*, vol. 81, pp. 994–1001, 2018.

[10] A. Youssef, M. E. Telbany, A. Zekry, and A. Zekry, "Reconfigurable generic FPGA implementation of fuzzy logic controller for MPPT of PV systems," *Renewable and Sustainable Energy Reviews*, vol. 82, pp. 1313–1319, 2018.

[11] X. Li, H. Wen, Y. Hu, and L. Jiang, "A novel beta parameter based fuzzy-logic controller for photovoltaic MPPT application," *Renewable Energy*, vol. 130, pp. 416–427, 2019.

[12] M. Arjun and J. B. Zubin, "Artificial neural network based hybrid MPPT for photovoltaic modules," in *Proceedings of the 2018 International CET Conference on Control, Communication, and Computing (IC4)*, pp. 140–145, Thiruvananthapuram, India, 2018.

[13] S. Messalti, A. Harrag, and A. Loukriz, "A new variable step size neural networks MPPT controller: review, simulation and hardware implementation," *Renewable and Sustainable Energy Reviews*, vol. 68, pp. 221–233, 2017.

[14] N. A. Kamal, A. T. Azar, G. S. Elbasuony, K. M. Almustafa, and D. Almakhles, "PSO-based adaptive Perturb and Observe MPPT technique for photovoltaic systems," in *Proceedings of the International Conference on Advanced Intelligent Systems and Informatics*, pp. 125–135, 2019.

[15] K. Prasad Panda, A. Anand, P. Ranjan Bana, and G. Panda, "Novel PWM control with modified PSO-MPPT algorithm for reduced switch MLI based standalone PV system," *International Journal of Emerging Electric Power Systems*, vol. 19, p. 5, 2018.

[16] M. Zhang, Z. Chen, and L. Wei, "An immune firefly algorithm for tracking the maximum power point of PV array under partial shading conditions," *Energies*, vol. 12, no. 16, p. 3083, 2019.

[17] S. Hadji, J.-P. Gaubert, and F. Krim, "Real-time genetic algorithms-based mppt: study and comparison (theoretical an experimental) with conventional methods," *Energies*, vol. 11, p. 459, 2018.

[18] M. Y. Javed, A. F. Murtazab, Q. Linga, S. Qamara, and M. Majid Gulzar, "A novel MPPT design using generalized pattern search for partial shading," *Energy and Buildings*, vol. 133, pp. 59–69, 2016.

[19] B. Yang, L. Zhong, X. Zhang et al., "Novel bio-inspired memetic salp swarm algorithm and application to MPPT for PV systems considering partial shading condition," *Journal of Cleaner Production*, vol. 215, pp. 1203–1222, 2019.

[20] A. A. Z. Diab, "MPPT of PV system under partial shading conditions based on hybrid whale optimization-simulated annealing algorithm (WOSA)," in *Modern Maximum Power Point Tracking Techniques for Photovoltaic Energy Systems*, pp. 355–378, Springer, Berlin, Germany, 2020.

[21] D. G. Montgomery, *Design and Analysis of Experiments*, Wiley, Hoboken, NJ, USA, 5 edition, 2001.

[22] O. Abdalla, H. Rezk, and E. M. Ahmed, "Wind driven optimization algorithm based global MPPT for PV system under non-uniform solar irradiance," *Solar Energy*, vol. 180, pp. 429–444, 2019.

[23] M. Taherkhani, J. Faraji, M. Khanjanianpak, E. Aliyan, and M. I. Ghiyasi, "A GMPPT design using the following optimization algorithm for PV systems," *International Transactions on Electrical Energy Systems*, vol. 31, no. 7, Article ID e12794, 2021.

[24] B. Korich, A. Benaissa, B. Rabhi, and D. Bakria, "A novel MPPT design for a partially shaded PV system using spotted Hyena optimization algorithm," *Engineering, Technology & Applied Science Research*, vol. 11, no. 6, pp. 7776–7781, 2021.

[25] C. Ghenai, A. Merabet, T. Salameh, and E. Pigem, "Grid-tied and stand-alone hybrid solar power system for desalination," *Desalination*, vol. 435, pp. 172–180, 2018.

[26] A. Mathew and A. I. Selvakumar, "MPPT based stand-alone water pumping system," in *Proceedings of the 2011 International Conference on Computer, Communication and Electrical Technology (ICCCET)*, Tirunelveli, India, 2011.

[27] P. Kofinas, A. I. Dounis, G. Papadakis, and M. N. Assimakopoulos, "An Intelligent MPPT controller based on direct neural control for partially shaded PV system," *Energy and Buildings*, vol. 90, pp. 51–64, 2015.

[28] A. Chaouachi, R. M. Kamel, and K. Nagasaka, "A novel multi-model neuro-fuzzy-based MPPT for three-phase grid-connected photovoltaic system," *Solar Energy*, vol. 84, no. 12, pp. 2219–2229, 2010.

[29] X. Li, R. Rakkiyappan, and P. Balasubramaniam, "Existence and global stability analysis of equilibrium of fuzzy cellular neural networks with time delay in the leakage term under impulsive perturbations," *Journal of the Franklin Institute*, vol. 348, no. 2, pp. 135–155, 2011.

[30] K. Y. Kuo and J. Lin, "Fuzzy logic control for flexible link robot arm by singular perturbation approach," *Applied Soft Computing*, vol. 2, no. 1, pp. 24–38, 2002.

[31] C. H. Lien, K. W. Yu, H. C. Chang, L. Y. Chung, and J. D. Chen, "Robust reliable guaranteed cost control for uncertain T-S fuzzy neutral systems with interval time-varying delay and linear fractional perturbations," *Optimal Control Applications and Methods*, vol. 36, no. 1, pp. 121–137, 2015.

[32] M. Mendel Jerry, *Uncertain Rule-Based Fuzzy Logic System: Introduction and New Directions*, Springer, Berlin, Germany, 2001.

[33] M. I. Bahari, P. Tarassodi, Y. M. Naeini, A. K. Khalilabad, and P. Shirazi, "Modeling and simulation of hill climbing MPPT algorithm for photovoltaic application," in *Proceedings of IEEE International Symposium on Power Electronics, Electrical*

Drives, Automation and Motion (SPEEDAM), pp. 1041–1044, Capri, Italy, 2016.

[34] M. Miyatake, M. Veerachary, F. Toriumi, N. Fujii, and H. Ko, "Maximum power point tracking of multiple photovoltaic arrays: a PSO approach," *IEEE Transactions on Aerospace and Electronic Systems*, vol. 47, no. 1, pp. 367–380, 2011.

[35] K. shaque, Z. Salam, M. Amjad, and S. Mekhilef, "An improved particle swarm optimization (PSO)–based MPPT for PV with reduced steady-state oscillation," *IEEE Transactions on Power Electronics*, vol. 27, no. 8, pp. 3627–3638, 2012.

[36] H. Renaudineau, F. Donatantonio, J. Fontchastagner et al., "A PSO-based global MPPT technique for distributed PV power generation," *IEEE Transactions on Industrial Electronics*, vol. 62, no. 2, pp. 1047–1058, 2015.

[37] H. Yang, W. Zhou, L. Lu, and Z. Fang, "Optimal sizing method for stand-alone hybrid solar–wind system with LPSP technology by using genetic algorithm," *Solar Energy*, vol. 82, no. 4, pp. 354–367, 2008.

[38] C. Larbes, S. A. Cheikh, T. Obeidi, and A. Zerguerras, "Genetic algorithms optimized fuzzy logic control for the maximum power point tracking in photovoltaic system," *Renewable Energy*, vol. 34, no. 10, pp. 2093–2100, 2009.

[39] A. Panda, M. K. Pathak, and S. P. Srivastava, "Fuzzy intelligent controller for the maximum power point tracking of a photovoltaic module at varying atmospheric conditions," *Journal of Energy Technologies and Policy*, vol. 1, no. 2, pp. 18–27, 2011.

[40] B. Bendib, F. Krim, H. Belmili, M. F. Almi, and S. Boulouma, "Advanced fuzzy MPPT controller for a stand-alone PV system," *Energy Procedia*, vol. 50, pp. 383–392, 2014.

[41] C. S. Chiu and Y. L. Ouyang, "Robust maximum power tracking control of uncertain photovoltaic systems: a unified TS fuzzy model-based approach," *IEEE Transactions on Control Systems Technology*, vol. 19, no. 6, pp. 1516–1526, 2011.

[42] A. El Khateb, N. A. Rahim, J. Selvaraj, and M. N. Uddin, "Fuzzy-logic-controller-based SEPIC converter for maximum power point tracking," *IEEE Transactions on Industry Applications*, vol. 50, no. 4, pp. 2349–2358, 2014.

[43] T. A. Ocran, J. Cao, B. Cao, and X. Sun, "Artificial neural network maximum power point tracker for solar electric vehicle," *Tsinghua Science and Technology*, vol. 10, no. 2, pp. 204–208, 2005.

[44] A. B. G. Bahgat, N. H. Helwa, G. E. Ahmad, and E. T. El Shenawy, "Maximum power point traking controller for PV systems using neural networks," *Renewable Energy*, vol. 30, no. 8, pp. 1257–1268, 2005.

[45] R. Ramaprabha, B. L. Mathur, and M. Sharanya, "Solar array modeling and simulation of MPPT using neural network," in *Proceedings of IEEE International Conference on Control, Automation, Communication and Energy Conservation, INCACEC*, pp. 1–5, Perundurai, India, 2009.

[46] A. M. Kassem, "MPPT control design and performance improvements of a PV generator powered DC motor-pump system based on artificial neural networks," *International Journal of Electrical Power & Energy Systems*, vol. 43, no. 1, pp. 90–98, 2012.

[47] S. Daraban, D. Petreus, and C. Morel, "A novel MPPT (maximum power point tracking) algorithm based on a modified genetic algorithm specialized on tracking the global maximum power point in photovoltaic systems affected by partial shading," *Energy*, vol. 74, pp. 374–388, 2014.

[48] G. Komarasamy and A. Wahi, "An optimized K-means clustering technique using bat algorithm," *European Journal of Scientific Research*, vol. 84, no. 2, pp. 263–273, 2012.

[49] E. Lodhi, F. Y. Wang, G. Xiong et al., "A dragonfly optimization algorithm for extracting maximum power of grid-interfaced PV systems," *Sustainability*, vol. 13, no. 19, Article ID 10778, 2021.

[50] M. Sultan, J. Wu, F. Aleem, and M. Imran, "Cost and energy analysis of a grid tie solar system synchronized with utility and fossil fuel generation with major issues for the attenuation of solar power in Pakistan," *Solar Energy*, vol. 174, pp. 967–975, 2018.

[51] F.. Keyrouz, "Enhanced Bayesian based MPPT controller for PV systems," *IEEE Power and Energy Technology Systems Journal*, vol. 5, no. 1, pp. 11–17, 2018.

[52] H. Tian, F. Mancilla-David, K. Ellis, E. Muljadi, and P. Jenkins, "Determination of the optimal configuration for a photovoltaic array depending on the shading condition," *Solar Energy*, vol. 95, pp. 1–12, 2013.

[53] M. K. Karagöz and H. Demirel, "Novel MPPT method for PV arrays based on modified bat algorithm with partial shading capability," *Int. J. Comput. Sci. Netw. Secur*, vol. 17, pp. 61–66, 2017.

[54] R. Jin, W. Chen, and A. Sudjianto, "On sequential sampling for global metamodeling in engineering design," in *Proceedings of the ASME 2002 International Design Engineering Technical Conferences and Computers and Information in Engineering Conference*, Montreal, Quebec, Canada, 2002.

[55] S. Cheng, J. Zhou, and M. Li, "A new hybrid algorithm for multi-objective robust optimization with interval uncertainty," *Journal of Mechanical Design*, vol. 137, no. 2, Article ID 021401, 2015.

[56] A. M. Eltamaly, "A novel musical chairs algorithm applied for MPPT of PV systems," *Renewable and Sustainable Energy Reviews*, vol. 146, Article ID 111135, 2021.

[57] S. Shan and G. G. Wang, "An efficient Pareto set identification approach for multiobjective optimization on black-box functions," *Journal of Mechanical Design*, vol. 127, no. 5, pp. 866–874, 2005.